A Bayesian ranking statistic to find high-mass black holes in LIGO data

A. Vajpeyi[1,2], R. Smith[1,2], E. Thrane[1,2], G. Ashton[1,2], J. Kanner[3], T. Alford[3], L. Xiao[3], M. Isi[4,5], S. Garza[3],

[1]School of Physics and Astronomy, Monash University, Clayton VIC 3800, Australia
[2]OzGrav: The ARC Centre of Excellence for Gravitational Wave Discovery, Clayton VIC 3800, Australia
[3]LIGO Laboratory, California Institute of Technology, Pasadena, CA 91125, USA
[4]LIGO Laboratory, Massachusetts Institute of Technology, Cambridge, MA 02139, USA
[5]Department of Physics and Kavli Institute for Astrophysics and Space Research, Massachusetts Institute of Technology, 77 Massachusetts Ave, Cambridge, MA 02139, USA

(Dated: January 28, 2021)

The detection of intermediate-mass black holes ($10^2 - 10^6$ $M_\odot$) will shed light on the formation of supermassive black holes and thus galaxy formation. Although LIGO is sensitive to the merger of binary black holes with total masses up to 400 $M_\odot$, only 4 of their 50 detections have a total mass > 100 $M_\odot$. A possible explanation for the absence of intermediate-mass events may be their misclassification as short-duration instrumental noise transients. Short-duration instrumental transients mimic the short-duration gravitational-wave signals from intermediate-mass binary black hole mergers. Here we demonstrate that a ranking statistic utilising Bayesian inference could be a more sensitive tool for detecting high-mass binary black hole mergers (systems with a total mass > 55 $M_\odot$) compared to a traditional match-filter ranking statistic. We applied this technique on the high-mass triggers during LIGO's second observing run to investigate the possibility of discovering new gravitational-wave signals from high mass black hole binaries and re-calculate the significance of high-mass candidate events. Although our analysis does not discover new gravitational wave events, it does provide a Bayesian measure of various candidates and events.

I. INTRODUCTION

Since the 1970s, there has been an accumulation of evidence for stellar-mass and supermassive black holes. In April 2019, the Event Horizon Telescope provided the first visual evidence of the supermassive black hole M87 [1]. As of January 2021, the LIGO Scientific Collaboration has confirmed ~ 50 binary black hole systems and listed numerous candidate events [2–4]. Additionally, since the public release of LIGO's first and second observing run's data (O1 and O2), several external groups, such as `PyCBC` [5] and a research team at the Institute for Advanced Study (IAS) [6–8], have independently searched and identified additional binary black hole gravitational wave candidates. These various discoveries have firmly authenticated the existence of stellar-mass black holes, supermassive black holes and binary black hole systems.

Until recently, there was no definitive evidence for intermediate-mass black holes, the black holes whose masses lie between that of stellar-mass and supermassive black hole systems ($10^2 - 10^6$ $M_\odot$). This changed with the detection of GW190521, a unique gravitational wave event that led to the formation of a black hole with a mass 142 $M_\odot$, the first confirmed direct discovery of an intermediate-mass black hole [9]. Although this is the first gravitational wave event leading to discovering a black hole with a mass in the intermediate range, ground-based gravitational wave detectors are sensitive to gravitational waves from even more massive systems to systems with a total mass of 400 $M_\odot$. [AV: double check the following – is this the most recent rate quote?] Additionally, gravitational waves from systems with masses greater than 100 $M_\odot$ systems should occur at a rate of $0 - 10\text{yr}^{-1}$ [10–13]. Hence, LIGO might have gravitational wave events from more intermediate-mass systems hidden in its data, potentially even in O2 data.

However, even after conducting a targeted matched-filter based search for gravitational waves from intermediate-mass black holes in O2's data, the heaviest total mass detected so far is approximately 80 $M_\odot$ [2, 13, 14]. A possible explanation for the absence of intermediate-mass events may be due to their misclassification as short-duration instrumental noise transients known as glitches [15–17]. These glitches can mimic astrophysical signals and hence decrease the significance of true gravitational wave events.

One method to account for glitches while searching for gravitational waves from coalescing compact binaries is by utilising an astrophysical Bayesian odds [18–22]. A true Bayesian odds calculated without using bootstrap techniques can provide events with a more accurate significance that is agnostic to a specific search strategy [20–22].

Additionally, Bayesian odds can include comprehensive astrophysical information in its calculation. For example, a Bayesian odds to help detect gravitational-wave candidates can incorporate information on if an event's binary system was precessing and if the signal contains higher-order modes and is coherent amongst various detectors. Because of the possibility of Bayesian methods to incorporate detailed physical information about

a gravitational wave signal, the LIGO Scientific Collaboration uses Bayesian methods to determine the source parameters of gravitational-wave events [2, 23]. This paper demonstrates that the power of Bayesian methods used in parameter estimation can also discriminate between coherent gravitational-wave signals, incoherent glitches, and Gaussian noise in the form of a Bayesian odds, utilised as a ranking statistic.

In this paper, we utilise a Bayesian method, called the Bayesian Coherence Ratio $\rho_{\rm BCR}$ [19], to rank the candidate gravitational wave signals from high-mass compact binary coalescences (systems with total masses in the range of $55 - 500$ $\rm M_{\odot}$) in the detector data recorded during O2. Although the $\rho_{\rm BCR}$, utilising bootstrap techniques, does not provide the true Bayesian odds, it provides a more astrophysical measure of candidate events' significance than a traditional match-filter significance.

We find that (a) high-mass events reported in the GWTC-1, including GW170729 (an event with disputed $p_{\rm astro}$ amongst various search pipelines) have high significance; (b) high-mass events detected from the IAS group have differing levels of significance; and that (c) our ranking statistic does not identify any intermediate-mass black holes, but does identify an unreported stellar-mass binary black hole candidate, 170222.

The remainder of this paper is structured as follows. We outline our methods, including details of the $\rho_{\rm BCR}$ and the retrieval of our candidate events in Section II. We present details on the implementation of our analysis in Section III. Finally, we present our results in Section IV, and discuss these results in the context of the significance of gravitational wave candidates in Section V.

II. METHOD

The gravitational wave community uses Bayesian inference to perform parameter estimation and model selection. In this work, we utilise Bayesian inference to calculate the significance of high-mass candidate events in O2 by using the $\rho_{\rm BCR}$ as a ranking statistic, taking a step toward building a unified Bayesian framework to search for candidates and estimate their parameters.

Although a dedicated Bayesian search for gravitational waves, as presented by Ashton *et al.* [20], does not require noise estimation using empirical methods, this Bayesian significance ranking technique utilises *time-slides*. To perform time-slides, data from independent observatories are time-shifted by amounts greater than the light-travel time between the two detectors. Each unique time-slide amount creates an artificial signal-free 'background' data set. When search pipelines scan these background data sets for gravitational wave events, they can find *triggers*[1], even though the background data set should not contain coherent astrophysical signals. These triggers in background data are labelled background triggers, while coherent triggers obtained in non-time-slid data are labelled candidate triggers.

Calculating the $\rho_{\rm BCR}$ ranking statistic for each background trigger builds a background $\rho_{\rm BCR}$ distribution. With a background distribution, it is possible to assign a statistical significance of how likely a candidate trigger, detected by the search pipelines over non-time slid data, is due to a gravitational wave signal.

This section discusses (a) the method to retrieve triggers, and (b) the $\rho_{\rm BCR}$ and how it is utilised as a ranking statistic to calculate the significance of candidate triggers.

A. Triggers for Analysis

The LIGO Scientific collaboration operates several search pipelines that scan for gravitational waves from compact binary mergers such as `GstLAL`, `MBTA`, `SPIIR` and `PyCBC` [2].

The output of `PyCBC`'s search is a list of candidate trigger times and their corresponding `PyCBC` ranking statistic $\rho_{\rm PC}$. The $\rho_{\rm PC}$ statistic is akin to the matched-filter signal-to-noise ratio ρ. However, unlike ρ, $\rho_{\rm PC}$ includes some information on the candidate signal's intrinsic and extrinsic properties and other information that feeds into determining if the signal can have astrophysical origins [25]. The additional physical information incorporated in $\rho_{\rm PC}$ makes it a more accurate measure of significance than the standard ρ.

Whenever a local maximum of $\rho_{\rm PC} > \rho_{\rm T}$, where $\rho_{\rm T}$ is some threshold value, the `PyCBC` search pipeline produces a single-detector trigger associated with the detector and time where the apparent signal in the data has its merger [25].

For `PyCBC` to consider a trigger to be a *candidate trigger*, a trigger that may be from astrophysical origins, the trigger must be observed between detectors with the same template and a time of arrival difference less than the gravitational-wave travel time [24]. To test its search, `PyCBC` also conducts searches for *simulated triggers*, artificial triggers manufactured by injecting signals into the detector data. These simulated signal studies provide `PyCBC` with metrics on its search's sensitivity. Finally, to quantify the statistical significance of candidate events, `PyCBC` artificially constructs a *background trigger* set to compare against the candidate events. These background triggers are coherent signal-free events, constructed by applying relative offsets, or time-slides, between the data of different detectors [25]. The time-slides to generate the background triggers are greater than the gravitational-wave travel time between detectors to ensure that the background triggers are not of astrophysical origins.

[2] *Triggers* are points in time when the matched-filter SNR is larger than a threshold value for a given gravitational wave template [24].

Our work demonstrates that the $\rho_{\rm BCR}$ can be used in the same way as $\rho_{\rm PC}$ to measure candidate triggers' statistical significance. The $\rho_{\rm BCR}$ can be a powerful ranking statistic as the $\rho_{\rm BCR}$ incorporates information of not only all possible binary black hole systems that might have merged to produce the trigger but also the various incoherent glitches that might cause a false-detection.

Before we discuss how we use the $\rho_{\rm BCR}$ as a measure of significance, we introduce the method to calculate the $\rho_{\rm BCR}$ in the following section.

B. The Bayesian Coherence Ratio

Bayes theorem states that the posterior probability distribution $p(\vec{\theta}|d,\mathcal{H})$ for data d and a vector of parameters $\vec{\theta}$ that describe a model which quantifies a hypothesis $\mathcal{H}$, is given by

$$p(\vec{\theta}|d,\mathcal{H}) = \frac{\mathcal{L}(d|\vec{\theta},\mathcal{H})\ \pi(\vec{\theta}|\mathcal{H})}{\mathcal{Z}(d|\mathcal{H})}\ , \tag{1}$$

where $\mathcal{L}(d|\vec{\theta},\mathcal{H})$ is the likelihood of the data given the parameters $\vec{\theta}$ and the hypothesis, $\pi(\vec{\theta}|\mathcal{H})$ is the prior probability of the parameters, and finally,

$$\mathcal{Z}(d|\mathcal{H}) = \int_{\vec{\theta}} \mathcal{L}(d|\vec{\theta},\mathcal{H})\ \pi(\vec{\theta}|\mathcal{H})\ d\vec{\theta} \tag{2}$$

is the likelihood after marginalising over the parameters $\vec{\theta}$. To compare two hypotheses $\mathcal{H}_A$ and $\mathcal{H}_B$ with the Bayes theorem one can calculate an odds ratio

$$\mathcal{O}^A_B = \frac{\mathcal{Z}^A\ \pi(\vec{\theta}^A)}{\mathcal{Z}^B\ \pi(\vec{\theta}^B)}\ , \tag{3}$$

where $\mathcal{Z}^A$ and $\mathcal{Z}^B$ are the shorthand for the evidences $\mathcal{Z}(d|\mathcal{H}_A)$ and $\mathcal{Z}(d|\mathcal{H}_B)$. The odds ratio can tell us which of the two hypotheses is more likely. For example, if $\mathcal{O}^A_B >> 1$, then this odds ratio indicates that the $\mathcal{H}_A$ describes the data much better than $\mathcal{H}_B$.

The $\rho_{\rm BCR}$ is a Bayesian odds ratio like the above, of a coherent signal hypotheses $\mathcal{H}_S$ and an incoherent instrumental feature hypothesis $\mathcal{H}_I$ for a network of D detectors. $\mathcal{H}_\mathcal{I}$ states that each detector i has either pure Gaussian noise $\mathcal{H}_N$ or a glitch $\mathcal{H}_G$. Following Isi *et al.* [19], the $\rho_{\rm BCR}$ is given by

$$\rho_{\rm BCR} = \frac{\alpha Z^S}{\prod_{i=1}^{D}\left[\beta Z^G_i + (1-\beta)Z^N_i\right]}\ , \tag{4}$$

where Z^S, Z^G_i and Z^N_i are the Bayesian evidences (marginalised likelihoods) for $\mathcal{H}_S$, $\mathcal{H}_N$, and $\mathcal{H}_G$. α and β, are the prior odds for obtaining a signal $\alpha = P(\mathcal{H}_S)/P(\mathcal{H}_I)$ and the prior odds for obtaining a glitch $\beta = P(\mathcal{H}_G)/P(\mathcal{H}_I)$. As the rate of signal and glitches are unknown, these priors α and β are tuned to maximise the $\rho_{\rm BCR}$ distributions for background data (coherent signal-free data) and simulated signals [19].

C. Bayesian Evidence Evaluation

1. Noise Model

We assume that each detector's noise is Gaussian and stationary over the period being analysed [26]. In practice, we assume that the noise has a mean of zero that the noise variance σ^2 is proportional to the noise power spectral density (PSD) $P(f)$ of the data. Using the $P(f)$, for each data segment d_i in each of the i detectors in a network of D detectors, we can write

$$Z^N_i = \mathcal{N}(d_i) = \frac{1}{2\pi P(f)_i}\ \exp\left(-\frac{1}{2}\frac{d_i}{P(f)_i}\right)\ , \tag{5}$$

where $\mathcal{N}(d_i)$ is a normal distribution with $\mu = 0$ and $\sigma^2 \sim P(f)$.

2. Coherent Signal Model

We model coherent signal using a binary black hole waveform template $\mu(\vec{\theta})$, where the vector $\vec{\theta}$ contains a point in the 15 dimensional space describing precessing binary-black hole mergers. For the signal to be coherent, $\vec{\theta}$ must be consistent in each 4-second data segment d_i for a network of D detectors, Hence, the coherent signal evidence is calculated as

$$Z^S = \int_{\vec{\theta}} \prod_{i=1}^{D}\left[\mathcal{L}(d_i|\mu(\vec{\theta}))\right]\pi(\vec{\theta}|\mathcal{H}_S)\ {\rm d}\vec{\theta}\ , \tag{6}$$

where $\pi(\vec{\theta}|\mathcal{H}_S)$ is the prior for the parameters in the coherent signal hypothesis, and $\mathcal{L}(d_i|\mu(\vec{\theta})))$ is the likelihood for the coherent signal hypothesis that depends on the gravitational wave template $\mu(\vec{\theta})$ and its parameters $\vec{\theta}$.

3. Incoherent Glitch Model

Finally, as glitches are challenging to model and poorly understood, we utilise a surrogate model for glitches: the glitches are modelled using gravitational wave templates $\mu(\vec{\theta})$ with uncorrelated parameters amongst the different detectors such that $\vec{\theta}_i \neq \vec{\theta}_j$ for two detectors i and j [18]. Modelling glitches with $\mu(\vec{\theta})$ captures the worst case scenario: when glitches appear similar to gravitational wave signals. Thus, we can write Z^G_i as

$$Z^G_i = \int_{\vec{\theta}} \mathcal{L}(d_i|\mu(\vec{\theta}))\ \pi(\vec{\theta}|\mathcal{H}_G)\ {\rm d}\vec{\theta}\ , \tag{7}$$

where $\pi(\theta|\mathcal{H}_G)$ is the prior for the parameters in the incoherent glitch hypothesis.

D. Tuning the BCR

After calculating the $\rho_{\rm BCR}$ for a set of background triggers and simulated triggers from as stretch of detector-data (a data chunk), we can compute probability distributions for the background and simulated triggers, $p_b(\rho_{\rm BCR})$ and $p_s(\rho_{\rm BCR})$. We expect the background trigger and simulated signal $\rho_{\rm BCR}$ values to favour the incoherent glitch and the coherent signal hypothesis, respectively. Ideally, these distributions representing two unique populations should be distinctly separate and have no overlap in their $\rho_{\rm BCR}$ values. The prior odds parameters α and β from Eq. 4 help separate the two distributions. Altering α translates the $\rho_{\rm BCR}$ probability distributions while adjusting β spreads the distributions. Although Bayesian hyper-parameter estimation can determine the optimal values for α and β, an easier approach is to adjust the parameters for each data chunk's $\rho_{\rm BCR}$ distribution. In this study, we tune α and β to maximally separate the $\rho_{\rm BCR}$ distributions for the background and simulated triggers.

To calculate the separation between $p_b(\rho_{\rm BCR})$ and $p_s(\rho_{\rm BCR})$, we use the Kullback–Leibler divergence (KL divergence) D_{KL}, given by

$$D_{KL}(p_b|p_s) = \sum_{x\in\rho_{\rm BCR}} p_b(x)\log\left(\frac{p_b(x)}{p_a(x)}\right) . \qquad (8)$$

The $D_{KL} = 0$ when the distributions are identical and increases as the asymmetry between the distributions increases.

We limit our search for the maximum KL-divergence in the α and β ranges of $[10^{-10}, 10^{0}]$ as values outside this range are nonphysical. We set our values for α and β to those which provide the highest KL-divergence and calculate the $\rho_{\rm BCR}$ for candidate events present in this data chunk. Note that we conduct the analysis in data chunks of a few days rather than an entire data set of a few months as the background may be different at different points of the entire data set.

E. Calculating the Significance of Candidate events

With the tuned values of α and β we can calculate the $\rho_{\rm BCR}$ for candidate events. As mentioned previously, irrespective of the Bayesian interpretation for $\rho_{\rm BCR}$, we treat the $\rho_{\rm BCR}$ as a traditional detection statistic to obtain a frequentist estimate of the significance of candidate event measured against the time-slid background $\rho_{\rm BCR}$ distribution.

We expect the background trigger $\rho_{\rm BCR}$ values to favour the incoherent glitch hypothesis (the null hypothesis). Candidate event $\rho_{\rm BCR}$ values will either be statistically insignificant compared to the background triggers, implying the candidate is a glitch, or statistically significant to the background distribution, indicating the possible presence of an astrophysical signal. To quantify the significance level, we can calculate a false alarm probability with trial factors FAP for the candidate events. The FAP is the probability that a candidate event originating from a non-astrophysical source can be is falsely identified as a signal.

To calculate the FAP, consider each candidate $\rho_{\rm BCR}$ as a single statistical trail that can occur at a fixed false alarm probability f, where f is the probability of observing a background $\rho_{\rm BCR}{}'$ greater than or equal to the candidate $\rho_{\rm BCR}$,

$$f = \frac{\text{Count of } \rho_{\rm BCR}{}' \leq \rho_{\rm BCR}}{\text{Count of } \rho_{\rm BCR}{}'} . \qquad (9)$$

The false alarm probability with trails FAP that the $\rho_{\rm BCR}$ measurement occurs at least once for N trials ($N > 0$), where N is the number of candidate triggers, can be written as

$$\text{FAP} = 1 - (1 - f)^N . \qquad (10)$$

The FAP can be used to construct a $p_{\rm astro}$, the probability that a signal is of astrophysical origin [27–29]

$$p_{\rm astro} = 1 - \text{FAP} . \qquad (11)$$

III. ANALYSIS

A. Acquisition of triggers

Advanced LIGO's second observing run O2 lasted 38 weeks [30]. The software package, `PyCBC` [5], processed the O2 data in 22 time-frames (approximately 2 weeks for one time-frames) and found several gravitational wave events and numerous gravitational wave candidates [24, 25, 31–35]. Some candidate events were vetoed to be glitches, while others were rejected due to their low significance. The data is divided into these time-frames because the detector's sensitivity does not stay constant throughout the eight-month-long observing period.

In addition to finding candidate events, `PyCBC` also identified several million background triggers for each time-frame, by searching background data manufactured by time-sliding data within that time-frame. The background triggers help quantify the candidate events' significance for the respective time-frames. Finally, to test the search's sensitivity, `PyCBC` produced and searched for thousands of simulated signals.

For our study, we filter the background, simulated and candidate events to include only high-mass events with masses in the ranges of the parameters presented in Table I. A plot of the `PyCBC` triggers from one time-frame, during April 23 - May 8, 2017, is presented in Figure 1. This figure also depicts the gravitational wave templates used during the search through this time-frame of data.

TABLE I. Template Banks's parameters for templates with duration < 454 ms.

	Minimum	Maximum
Component Mass 1 [$M_\odot$]	31.54	491.68
Component Mass 2 [$M_\odot$]	1.32	121.01
Total Mass [$M_\odot$]	56.93	496.72
Chirp Mass [$M_\odot$]	8.00	174.56
Mass Ratio	0.01	0.98

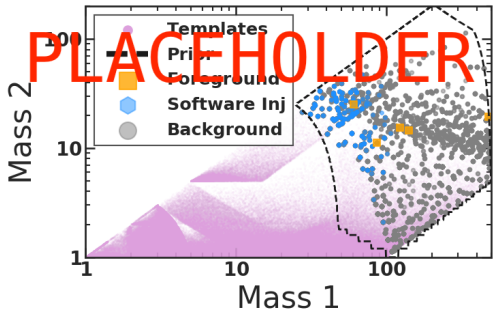

FIG. 1. The template bank used by PyCBC to search a section of O2 data from April 23 - May 8, 2017. Our search is constrained to the high-mass parameter space enclosed by the dashed line. [AV: Update plot]

B. Calculating the BCR for triggers

To evaluate Z^S, Z_i^G and Z_i^N as shown in Eqs. 5-7 and calculate the $\rho_{\rm BCR}$ Eq. 4 for these triggers, we carry out Bayesian inference with Bilby [36], employing dynesty [37] as our nested sampler. Nested sampling, an algorithm introduced by Skilling [38, 39], provides an estimate of the true Bayesian evidence and is often utilised for parameter estimation within the LIGO collaboration [36, 40, 41].

The most computationally intensive step during Bayesian inference is evaluating the likelihood $\mathcal{L}(d_i|\mu(\vec{\theta}))$. To accelerate our analysis, we use a likelihood that explicitly marginalises over coalescence time, phase at coalescence, and luminosity distance (Eq. 80 from Thrane and Talbot [42]). While this marginalised likelihood reduces the run time without introducing errors to our evidence evaluation, it does not generates samples for the marginalised parameters. However, these parameter samples can be calculated as a post-processing step [42].

We set the priors $\pi(\vec{\theta}|\mathcal{H}_S)$ and $\pi(\vec{\theta}|\mathcal{H}_G)$ to be identical. These priors restrict signals with mass parameters in the ranges presented in Table I. The spins are aligned over a uniform range for the dimensionless spin magnitude from $[0, 1]$. The luminosity distance prior assigns probability uniformly in comoving volume, with an upper cutoff of 5 Gpc. The full list of the priors, along with their shapes, limits and boundary conditions are documented in Table II.

The waveform template we utilise is IMRPhenomPv2, a phenomenological waveform template constructed in the frequency domain that models the inspiral, merger, and ringdown (IMR) of a compact binary coalescence [44]. Although gravitational wave templates such as SEOBNRv4PHM [45] which incorporate more physics, such as information on higher-order modes, we still use IMRPhenomPv2 as it is inexpensive compared to waveforms fitted against numerical-relativity simulations.

TABLE II. Prior settings for the parameters used during our parameter estimation. The definitions of the parameters are documented in Romero-Shaw *et al.* [43] Table E1.

Parameter	Shape	Limits	Boundary
$\mathcal{M}/M_\odot$	Uniform	7–180	Reflective
q	Uniform	0.1–1	Reflective
$M/M_\odot$	Constraint	50–500	–
$d_{\rm L}$/Mpc	Comoving	100–5000	Reflective
a_1, a_2	Uniform	0–1	Reflective
θ_{JN}	Sinusoidal	0–π	Reflective
ψ	Uniform	0–π	Periodic
ϕ	Uniform	0–2π	Periodic
ra	Uniform	0–2π	Periodic
dec	Cosine	0–2π	Reflective

We take 31 neighbouring, off-source, non-overlapping, 4-second segments of time-series data before the analysis data segment d_i to generate the PSD. We use off-source to avoid the inclusion of a signal in the PSD calculation. A Tukey window with 0.2-second roll-offs is applied to each data segment to suppress spectral leakage after which the segments are fast-Fourier transformed and median-averaged to create a PSD [26]. Like other PSD estimation methods, this method adds statistical uncertainties to the PSD [46, 47]. To marginalise over the statistical uncertainty, we use the median-likelihood presented by Talbot and Thrane [46] as a post-processing step and shift our Bayesian Evidence estimations closer to their astrophysical values.

Finally, we neglect detector calibration uncertainty and acquire data from from the Gravitational Wave Open Science Center [30]. The data we use is the publicly accessible O2 strain data from the Hanford and Livingston detectors, recorded while the detectors are in "Science Mode". We obtain the data using GWpy [48].

The run-time to calculate a single Bayesian evidence after using dynesty with $1,000$ live points and 100 walkers is usually between $1-12$ hours (where the run time is proportional to the SNR of the data segment). bilby_pipe orchestrates the creation of the PSDs and execution of the parameter estimation jobs [49].

C. Assigning $p_{\rm astro}$ to candidate events

After the calculating the $\rho_{\rm BCR}$ for the entire set of high-mass background and simulated triggers, we calculate probability distributions $p_b(\rho_{\rm BCR})$ and $p_s(\rho_{\rm BCR})$ for each 2-week time-frame of O2 data. These distributions are used to obtain the 'tuned' prior-odd α and β values

that maximise $D_{KL}(p_b|p_s)$ for each time-frame of data.

Finally, using the tuned prior odds the $\rho_{\rm BCR}$ for the candidate events can be calculated. Figure 2 shows the $\rho_{\rm BCR}$ distributions for the background triggers, simulated triggers and candidate events. The bulk of the background and simulated trigger distributions are separate but slightly overlap due to some of the simulated signal's being very faint. The separation suggests that the $\rho_{\rm BCR}$ can successfully distinguish signals from noise or glitches. The vertical lines in Figure 2 displays the $\rho_{\rm BCR}$ for gravitational wave candidate events. On comparing the candidate event $\rho_{\rm BCR}$ values with the background distribution, we can estimate $p_{\rm astro}$ values for the candidate events.

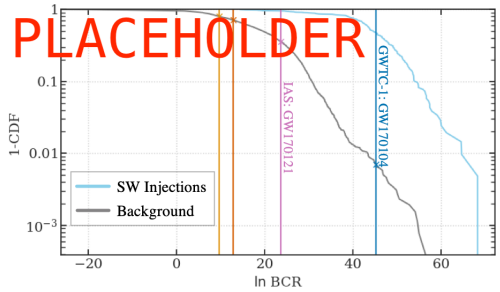

FIG. 2. Histograms represent the survival function (1-CDF) from our selection of ∼ 3,000 background triggers (grey) and 648 simulated signals (blue) triggers obtained from PyCBC's search of data from April 23 - May 8, 2017. [AV: change BCR to$\rho_{\rm BCR}$ in axes labels]Vertical lines mark the ln BCRs of two glitches (orange and yellow), IAS's GW170121 (pink), and GWTC-1's GW170104 (dark blue) [AV: this plot also doesn't add much, is it needed?].

IV. RESULTS

We analyse the 60 996 background, 5 146 simulated, and 25 candidate triggers reported by PyCBC's search of the data from the second observing run, restricting our analysis to the triggers that fall within our Bayesian prior space as described in Section II. In addition to these triggers, we also analyse events and candidate events reported by GWTC-1 and the IAS group (note that some of these were identified as candidates by the PyCBC search). In Table III, we summarise the $p^{\rm BCR}_{\rm astro}$, along with the $p_{\rm astro}$ of other pipelines for comparison. Note that although the various pipeline $p_{\rm astro}$ are not mathematically equivalent, by comparing pipeline $p_{\rm astro}$ values for a given event, we can compare how significant each pipeline deems various candidates. The α and β values utilised for each time-frame of O2 are reported in Appendix A

A. GWTC-1 Events

All the confirmed gravitational wave events from binary black hole mergers reported in GWTC-1 and within our prior space, (specifically GW170104, GW170608, GW170729, GW170809 and GW170814), have $p^{\rm BCR}_{\rm astro}$ greater than 0.9, indicating a high probability of the presence of an astrophysical signal.

In addition to the above confirmed gravitational wave events from GWTC-1, we have also analysed several candidate events discussed in GWTC-1, most of which have low $p^{\rm BCR}_{\rm astro}$. For example, consider the candidate event 170412, assigned a $p_{\rm astro}$ of 0.06 by GstLAL and has a $p^{\rm BCR}_{\rm astro}$ of 0.01. This candidate was reported to be excess power caused due noise appearing non-stationary between 60-200 Hz [2]. This candidate acts as an example of how $p^{\rm BCR}_{\rm astro}$ may be utilised to eliminate terrestrial noise sources, in addition to detecting signals

B. IAS Events

Our analysis of the high-mass IAS events and candidates in O2 has resulted in three events with disfavourable $p^{\rm BCR}_{\rm astro} < 0.5$ (GWC170402, GW170403, GW170425), and four events and one candidate with $p^{\rm BCR}_{\rm astro} \geq 0.5$ (GW170121, 170302, GW170304, GW170727, GW170817A).

GWC170402, detected by Zackay *et al.* [8], is reported to have a signal that is not described well by waveforms for circular binaries with aligned spins. Hence, we might have received a low $p^{\rm BCR}_{\rm astro}$ due to our usage of IMRPhenomPv2, a waveform that does not account for eccentricity. Additionally, the search conducted by Zackay *et al.* [8] was a single-detector search. Our ranking statistic relies on the signal to appear coherent, even if just faintly coherent, amongst the various detectors to have a high $p^{\rm BCR}_{\rm astro}$. Hence, the lack of coherence and the non-eccentric waveform may be the leading factors for a low $p_{\rm astro}$. GW170403 and GW170425 which have $p^{\rm BCR}_{\rm astro} < 0.35$ also have low $p_{\rm astro}$ reported by Nitz *et al.* [50], suggesting that these events may have been false alarms.

From the candidates with $p^{\rm BCR}_{\rm astro} > 0.5$, GW170727 and 170302 are of particular interest, with $p^{\rm BCR}_{\rm astro}$ of 0.92 and 0.63. GW170727 was emitted from a black hole binary system with a source frame total mass $\approx 70\ {\rm M}_\odot$. In addition to the high $p^{\rm BCR}_{\rm astro}$ reported by our study, Venumadhav *et al.* [7] and Nitz *et al.* [50] have also reported high $p_{\rm astro}$ values of 0.98 and 0.99, making it a viable gravitational-wave event candidate. Similarly, the sub-marginal-candidate 170302 reported by [7] with a $p_{\rm astro}$ of 0.45 appears to have a higher significance from our analysis, resulting in a $p^{\rm BCR}_{\rm astro}$ of 0.63.

TABLE III. The $p_{\rm astro}$ of gravitational wave events from various detection pipelines, along with the event candidates with $p^{\rm BCR}_{\rm astro} > 0.3$. Only the candidates and events within our prior space are displayed. The various pipeline $p_{\rm astro}$ represented in this table, $p^{\rm ext}_{\rm astro}$, are from the following pipelines: GstLAL $^{\heartsuit}$ [2], PyCBC $^{\spadesuit}$ [2], PyCBC OGC-2 $^{\clubsuit}$ [50], PyCBC 'single-search' $^{\blacklozenge}$ [51], IAS $^{\bigstar}$ [7, 8], and Pratten and Vecchio [22]'s significances $^{\blacktriangle}$. The catalogues labelled IAS-1 and IAS-2 correspond to the candidates published in Venumadhav *et al.* [7] and Zackay *et al.* [8].

Event	Catalogue	$p^{\rm BCR}_{\rm astro}$	$p^{\rm ext}_{\rm astro}$	GPS
GW170104	GWTC-1	0.94	$1.00^{\heartsuit}; 1.00^{\spadesuit}; 1.0^{\blacktriangle}$	1167559934.60
GW170121	IAS-1	0.76	$1.00^{\clubsuit}; 1.00^{\bigstar}; 0.53^{\blacktriangle}$	1169069152.57
170222	-	0.49	-	1171814474.97
170302	IAS-1	0.63	$0.45^{\bigstar}; 0.0^{\blacktriangle}$	1172487815.48
GW170304	IAS-1	0.83	$0.70^{\clubsuit}; 0.99^{\bigstar}; 0.03^{\blacktriangle}$	1172680689.36
GWC170402	IAS-2	0.38	$0.68^{\bigstar}; 0.03^{\blacklozenge}; 0.0^{\blacktriangle}$	1175205126.57
GW170403	IAS-1	0.33	$0.03^{\clubsuit}; 0.56^{\bigstar}; 0.27^{\blacktriangle}$	1175295987.22
GW170425	IAS-1	0.10	$0.21^{\clubsuit}; 0.77^{\bigstar}; 0.74^{\blacktriangle}$	1177134830.18
GW170608	GWTC-1	0.95	$0.92^{\heartsuit}; 1.00^{\spadesuit}; 1.0^{\blacktriangle}$	1180922492.50
GW170727	IAS-1	0.92	$0.99^{\clubsuit}; 0.98^{\bigstar}; 0.66^{\blacktriangle}$	1185152686.02
GW170729	GWTC-1	0.96	$0.98^{\heartsuit}; 0.52^{\spadesuit}; 1.0^{\blacktriangle}$	1185389805.30
GW170809	GWTC-1	0.98	$0.99^{\heartsuit}; 1.00^{\spadesuit}; 1.0^{\blacktriangle}$	1186302517.75
GW170814	GWTC-1	1.00	$1.00^{\heartsuit}; 1.00^{\spadesuit}; 1.0^{\blacktriangle}$	1186741859.53
GW170817A	IAS-2	0.83	$0.86^{\bigstar}; 0.36^{\blacklozenge}; 0.02^{\blacktriangle}$	1186974182.72

C. New Candidate Events

Although no clear detections are made with the $\rho_{\rm BCR}$, a marginal-candidate 170222 has been discovered with a $p^{\rm BCR}_{\rm astro} \sim 0.5$. This candidate has its similar masses when compared to those of GWTC-1. The remaining coherent trigger candidates all have $p^{\rm BCR}_{\rm astro} \ll 0.5$ making them unlikely to originate from astrophysical sources.

V. CONCLUSION

In this paper, we demonstrate that the Bayesian Coherence Ratio [19] can be used as a ranking statistic to provide a better measure of significance for gravitational wave candidates by re-analysing the significance of high-mass binary black hole triggers from O2. This method takes a step towards building a unified Bayesian framework that provides a search-pipeline agnostic measure of significance, utilising the same level of physical information incorporated during parameter estimation.

We focused our analysis on the high-mass regime as this region of the parameter space is plagued with a high number of short duration terrestrial artefacts that can mimic signals. In addition to the high-mass triggers, we also analyse the high-mass binary black hole events in O2 reported by LIGO [2] and IAS [7, 8]. Using $p^{\rm BCR}_{\rm astro}$, we find that the analysed GWTC-1 events have high probabilities of originating from an astrophysical source. We also find that some of the GWTC-1 marginal triggers that have corroborated terrestrial sources (for example candidate 170412) have low $p^{\rm BCR}_{\rm astro}$, indicating this method's ability to discriminate between terrestrial artefacts and astrophysical signals. Our analysis on the IAS events has demonstrated that GW17072 is highly likely to originate from an astrophysical source, while GW17040 is not. Finally, we did not identify any new gravitational-wave events, but we did find some a marginal candidate 170222.

Although our analysis targets high-mass triggers, this method can be extended to include the entire body range of LIGO-detectable gravitational wave sources. Additionally, to further improve the method's infrastructure, we can use more robust gravitational wave templates (such as templates that incorporate higher-order modes), and sophisticated glitch models. Future analysis can also incorporate data from all available detectors in a network to increase the sensitivity of $p^{\rm BCR}_{\rm astro}$. The BCR can discern better whether a candidate is a coherent astrophysical candidate or an incoherent glitch with data from more detectors.

[AV: as the core of this method is PE, improvements in PE can be adapted into this method]

ACKNOWLEDGMENTS

This research has made use of data, software and/or web tools obtained from the Gravitational Wave Open Science Center (https://www.gw-openscience.org), a ser-

TABLE IV. The prior odds used for each time-frame of data from O2. Each time frame commences at the start date and concludes at the following time-frame's start date.

Start Date	α	β
2016-11-15	-	-
2016-11-30	-	-
2016-12-23	-	-
2017-01-22	-	-
2017-02-03	1.00E-10	2.44E-01
2017-02-12	-	-
2017-02-20	6.55E-10	2.22E-03
2017-02-28	1.00E-10	5.96E-02
2017-03-10	2.56E-10	3.91E-01
2017-03-18	-	-
2017-03-27	-	-
2017-04-04	-	-
2017-04-14	1.05E-09	2.44E-01
2017-04-23	2.68E-09	1.46E-02
2017-05-08	-	-
2017-06-18	-	-
2017-06-30	2.02E-05	5.69E-03
2017-07-15	1.05E-09	9.54E-02
2017-07-27	-	-
2017-08-05	2.12E-04	3.73E-02
2017-08-13	2.68E-09	8.69E-04
2017-08-21	-	-

vice of LIGO Laboratory, the LIGO Scientific Collaboration and the Virgo Collaboration. LIGO is funded by the U.S. National Science Foundation. Virgo is funded by the French Centre National de Recherche Scientifique (CNRS), the Italian Istituto Nazionale della Fisica Nucleare (INFN) and the Dutch Nikhef, with contributions by Polish and Hungarian institutes.

Appendix A: Tuned prior odds

O2 lasted several months over which the detector's sensitivity varied. Hence, a part of our analysis entailed tuning the prior odds for obtaining a signal and a glitch, α and β, as described in Section II. Table IV presents the signal and glitch prior odds utilised for each time-frame of O2 data.

Tuning the prior odds can dramatically affect the $p_{\rm astro}^{\rm BCR}$. For example, consider Table V, which reports tuned $p_{\rm astro}^{\rm BCR}$ and un-tuned $p_{\rm astro}^{\rm BCR\prime}$ (where $\alpha = 1$ and $\beta = 1$) for various high-mass events and candidates. By tuning the prior odds, the $p_{\rm astro}^{\rm BCR}$ for some IAS events (for example, GW170403 and GW170817A) can change by more than 0.5, resulting in the promotion/demotion of a candidate's significance.

TABLE V. The BCR p-astro after tuning the prior odds, $p_{\rm astro}^{\rm BCR}$, and without tuning the prior odds, $p_{\rm astro}^{\rm BCR\prime}$.

Event	Catalogue	$p_{\rm astro}^{\rm BCR}$	$p_{\rm astro}^{\rm BCR\prime}$
161202	-	0.09	0.41
GW170104	GWTC-1	0.94	0.93
GW170121	IAS-1	0.76	0.72
170206	-	0.11	0.51
170222	-	0.49	0.48
170302	IAS-1	0.63	0.54
GW170304	IAS-1	0.83	0.81
GWC170402	IAS-2	0.38	0.01
GW170403	IAS-1	0.33	0.89
GW170425	IAS-1	0.10	0.22
GW170608	GWTC-1	0.95	0.95
GW170727	IAS-1	0.92	0.96
GW170729	GWTC-1	0.96	0.94
GW170809	GWTC-1	0.98	0.99
GW170814	GWTC-1	1.00	1.00
GW170817A	IAS-2	0.83	0.36

[1] Event Horizon Telescope Collaboration, K. Akiyama, A. Alberdi, W. Alef, *et al.*, First M87 Event Horizon Telescope Results. IV. Imaging the Central Supermassive Black Hole, ApJ **875**, L4 (2019), arXiv:1906.11241 [astro-ph.GA].

[2] B. P. Abbott, R. Abbott, T. D. Abbott, *et al.* (LIGO Scientific Collaboration and Virgo Collaboration), GWTC-1: A Gravitational-Wave Transient Catalog of Compact Binary Mergers Observed by LIGO and Virgo during the First and Second Observing Runs, Phys. Rev. X **9**, 031040 (2019).

[3] B. P. Abbott, R. Abbott, T. D. Abbott, *et al.*, GWTC-2: Compact Binary Coalescences Observed by LIGO and Virgo During the First Half of the Third Observing Run, arXiv e-prints , arXiv:2010.14527 (2020), arXiv:2010.14527 [gr-qc].

[4] GraceDB, Gravitational-Wave Candidate Event Database (2020).

[5] A. Nitz, I. Harry, D. Brown, C. M. Biwer, J. Willis, T. D. Canton, C. Capano, L. Pekowsky, T. Dent, A. R. Williamson, G. S. Davies, S. De, M. Cabero, B. Machenschalk, P. Kumar, S. Reyes, D. Macleod, F. Pannarale, dfinstad, T. Massinger, M. Tápai, L. Singer, S. Khan, S. Fairhurst, S. Kumar, A. Nielsen, shasvath, I. Dorrington, A. Lenon, and H. Gabbard, gwastro/pycbc: PyCBC Release 1.16.4 (2020).

[6] T. Venumadhav, B. Zackay, J. Roulet, L. Dai, and M. Zaldarriaga, New search pipeline for compact binary mergers: Results for binary black holes in the first observing run of Advanced LIGO, Physical Review D **100**, 023011 (2019).

[7] T. Venumadhav, B. Zackay, J. Roulet, L. Dai, and M. Zaldarriaga, New Binary Black Hole Mergers in the Second Observing Run of Advanced LIGO and Advanced Virgo, arXiv e-prints , arXiv:1904.07214 (2019), arXiv:1904.07214 [astro-ph.HE].

[8] B. Zackay, L. Dai, T. Venumadhav, J. Roulet, and M. Zaldarriaga, Detecting Gravitational Waves With Disparate Detector Responses: Two New Binary Black Hole Mergers, arXiv e-prints , arXiv:1910.09528 (2019), arXiv:1910.09528 [astro-ph.HE].

[9] B. P. Abbott, R. Abbott, T. D. Abbott, *et al.*, GW190521: A Binary Black Hole Merger with a Total Mass of 150 M_{odot}, Phys. Rev. Lett. **125**, 101102 (2020), arXiv:2009.01075 [gr-qc].

[10] J. M. Fregeau, S. L. Larson, M. C. Miller, R. O'Shaughnessy, and F. A. Rasio, Observing IMBH-IMBH binary coalescences via gravitational radiation, The Astrophysical Journal Letters **646**, L135 (2006).

[11] I. Mandel, D. A. Brown, J. R. Gair, and M. C. Miller, Rates and characteristics of intermediate mass ratio inspirals detectable by advanced LIGO, The Astrophysical Journal **681**, 1431 (2008).

[12] C. L. Rodriguez, M. Morscher, B. Pattabiraman, S. Chatterjee, C.-J. Haster, and F. A. Rasio, Binary black hole mergers from globular clusters: implications for Advanced LIGO, Physical Review Letters **115**, 051101 (2015).

[13] B. P. Abbott, R. Abbott, T. D. Abbott, *et al.* (LIGO Scientific Collaboration and Virgo Collaboration), Search for intermediate mass black hole binaries in the first and second observing runs of the Advanced LIGO and Virgo network, arXiv e-prints , arXiv:1906.08000 (2019), arXiv:1906.08000 [gr-qc].

[14] J. Aasi, B. Abbott, R. Abbott, T. Abbott, M. Abernathy, T. Accadia, F. Acernese, K. Ackley, C. Adams, T. Adams, *et al.*, Search for gravitational radiation from intermediate mass black hole binaries in data from the second LIGO-Virgo joint science run, Physical Review D **89**, 122003 (2014).

[15] A. H. Nitz, Distinguishing short duration noise transients in LIGO data to improve the PyCBC search for gravitational waves from high mass binary black hole mergers, Classical and Quantum Gravity **35**, 035016 (2018), arXiv:1709.08974 [gr-qc].

[16] J. Powell, Parameter estimation and model selection of gravitational wave signals contaminated by transient detector noise glitches, Classical and Quantum Gravity **35**, 155017 (2018), arXiv:1803.11346 [astro-ph.IM].

[17] M. Cabero, A. Lundgren, A. H. Nitz, T. Dent, D. Barker, E. Goetz, J. S. Kissel, L. K. Nuttall, P. Schale, R. Schofield, and D. Davis, Blip glitches in Advanced LIGO data, Classical and Quantum Gravity **36**, 155010 (2019), arXiv:1901.05093 [physics.ins-det].

[18] J. Veitch and A. Vecchio, Bayesian coherent analysis of in-spiral gravitational wave signals with a detector network, Phys. Rev. D **81**, 062003 (2010), arXiv:0911.3820 [astro-ph.CO].

[19] M. Isi, R. Smith, S. Vitale, T. J. Massinger, J. Kanner, and A. Vajpeyi, Enhancing confidence in the detection of gravitational waves from compact binaries using signal coherence, Phys. Rev. D **98**, 042007 (2018), arXiv:1803.09783 [gr-qc].

[20] G. Ashton, E. Thrane, and R. J. E. Smith, Gravitational wave detection without boot straps: A Bayesian approach, Phys. Rev. D **100**, 123018 (2019), arXiv:1909.11872 [gr-qc].

[21] G. Ashton and E. Thrane, The astrophysical odds of GW151216, MNRAS 10.1093/mnras/staa2332 (2020), arXiv:2006.05039 [astro-ph.HE].

[22] G. Pratten and A. Vecchio, Assessing gravitational-wave binary black hole candidates with Bayesian odds, arXiv e-prints , arXiv:2008.00509 (2020), arXiv:2008.00509 [gr-qc].

[23] B. Abbott, S. Jawahar, N. Lockerbie, and K. Tokmakov, LIGO Scientific Collaboration and Virgo Collaboration (2016) GW150914: first results from the search for binary black hole coalescence with Advanced LIGO. Physical Review D, 93 (12). ISSN 1550-2368, PHYSICAL REVIEW D Phys Rev D **93**, 122003 (2016).

[24] B. Allen, χ^2 time-frequency discriminator for gravitational wave detection, Phys. Rev. D **71**, 062001 (2005), arXiv:gr-qc/0405045 [gr-qc].

[25] G. S. Davies, T. Dent, M. Tápai, I. Harry, C. McIsaac, and A. H. Nitz, Extending the PyCBC search for gravitational waves from compact binary mergers to a global network, Phys. Rev. D **102**, 022004 (2020), arXiv:2002.08291 [astro-ph.HE].

[26] B. P. Abbott, R. Abbott, T. D. Abbott, *et al.*, A guide to LIGO-Virgo detector noise and extraction of transient gravitational-wave signals, arXiv e-prints , arXiv:1908.11170 (2019), arXiv:1908.11170 [gr-qc].

[27] W. M. Farr, J. R. Gair, I. Mandel, and C. Cutler, Counting and confusion: Bayesian rate estimation with multiple populations, Phys. Rev. D **91**, 023005 (2015), arXiv:1302.5341 [astro-ph.IM].

[28] S. J. Kapadia, S. Caudill, J. D. E. Creighton, W. M. Farr, G. Mendell, A. Weinstein, K. Cannon, H. Fong, P. Godwin, R. K. L. Lo, R. Magee, D. Meacher, C. Messick, S. R. Mohite, D. Mukherjee, and S. Sachdev, A self-consistent method to estimate the rate of compact binary coalescences with a Poisson mixture model, Classical and Quantum Gravity **37**, 045007 (2020), arXiv:1903.06881 [astro-ph.HE].

[29] S. M. Gaebel, J. Veitch, T. Dent, and W. M. Farr, Digging the population of compact binary mergers out of the noise, MNRAS **484**, 4008 (2019), arXiv:1809.03815 [astro-ph.IM].

[30] The LIGO Scientific Collaboration, the Virgo Collaboration, R. Abbott, T. D. Abbott, S. Abraham, F. Acernese, K. Ackley, C. Adams, R. X. Adhikari, V. B. Adya, and et al., Open data from the first and second observing runs of Advanced LIGO and Advanced Virgo, arXiv e-prints , arXiv:1912.11716 (2019), arXiv:1912.11716 [gr-qc].

[31] B. Allen, W. G. Anderson, P. R. Brady, D. A. Brown, and J. D. E. Creighton, FINDCHIRP: An algorithm for detection of gravitational waves from inspiraling compact binaries, Phys. Rev. D **85**, 122006 (2012), arXiv:gr-qc/0509116 [gr-qc].

[32] A. H. Nitz, T. Dent, T. Dal Canton, S. Fairhurst, and D. A. Brown, Detecting Binary Compact-object Mergers with Gravitational Waves: Understanding and Improving the Sensitivity of the PyCBC Search, ApJ **849**, 118 (2017), arXiv:1705.01513 [gr-qc].

[33] T. Dal Canton, A. H. Nitz, A. P. Lundgren, A. B. Nielsen, D. A. Brown, T. Dent, I. W. Harry, B. Krishnan, A. J. Miller, K. Wette, K. Wiesner, and J. L. Willis, Implementing a search for aligned-spin neutron star-black hole systems with advanced ground based gravitational wave detectors, Phys. Rev. D **90**, 082004 (2014), arXiv:1405.6731 [gr-qc].

[34] S. A. Usman, A. H. Nitz, I. W. Harry, C. M. Biwer, D. A. Brown, M. Cabero, C. D. Capano, T. Dal Canton, T. Dent, S. Fairhurst, M. S. Kehl, D. Keppel, B. Krishnan, A. Lenon, A. Lundgren, A. B. Nielsen, L. P. Pekowsky, H. P. Pfeiffer, P. R. Saulson, M. West, and J. L. Willis, The PyCBC search for gravitational waves from compact binary coalescence, Classical and Quantum Gravity **33**, 215004 (2016), arXiv:1508.02357 [gr-qc].

[35] A. H. Nitz, T. Dal Canton, D. Davis, and S. Reyes, Rapid detection of gravitational waves from compact binary mergers with PyCBC Live, Phys. Rev. D **98**, 024050 (2018), arXiv:1805.11174 [gr-qc].

[36] G. Ashton, M. Hübner, P. Lasky, and C. Talbot, Bilby: A User-Friendly Bayesian Inference Library (2019).

[37] J. S. Speagle, DYNESTY: a dynamic nested sampling package for estimating Bayesian posteriors and evidences, MNRAS **493**, 3132 (2020), arXiv:1904.02180 [astro-ph.IM].

[38] J. Skilling, Nested Sampling, in *Bayesian Inference and Maximum Entropy Methods in Science and Engineering: 24th International Workshop on Bayesian Inference and Maximum Entropy Methods in Science and Engineering*, American Institute of Physics Conference Series, Vol. 735, edited by R. Fischer, R. Preuss, and U. V. Toussaint (2004) pp. 395–405.

[39] J. Skilling, Nested sampling for general Bayesian computation, Bayesian Analysis **1**, 833 (2006).

[40] G. Ashton, M. Hübner, P. D. Lasky, C. Talbot, K. Ackley, S. Biscoveanu, Q. Chu, A. Divakarla, P. J. Easter, B. Goncharov, F. Hernandez Vivanco, J. Harms, M. E. Lower, G. D. Meadors, D. Melchor, E. Payne, M. D. Pitkin, J. Powell, N. Sarin, R. J. E. Smith, and E. Thrane, BILBY: A User-friendly Bayesian Inference Library for Gravitational-wave Astronomy, ApJS **241**, 27 (2019), arXiv:1811.02042 [astro-ph.IM].

[41] R. J. E. Smith, G. Ashton, A. Vajpeyi, and C. Talbot, Massively parallel Bayesian inference for transient gravitational-wave astronomy, MNRAS **498**, 4492 (2020), arXiv:1909.11873 [gr-qc].

[42] E. Thrane and C. Talbot, An introduction to Bayesian inference in gravitational-wave astronomy: Parameter estimation, model selection, and hierarchical models, PASA **36**, e010 (2019), arXiv:1809.02293 [astro-ph.IM].

[43] I. M. Romero-Shaw, C. Talbot, S. Biscoveanu, V. D'Emilio, G. Ashton, *et al.*, Bayesian inference for compact binary coalescences with BILBY: validation and application to the first LIGO-Virgo gravitational-wave transient catalogue, MNRAS **499**, 3295 (2020), arXiv:2006.00714 [astro-ph.IM].

[44] S. Khan, S. Husa, M. Hannam, F. Ohme, M. Pürrer, X. J. Forteza, and A. Bohé, Frequency-domain gravitational waves from nonprecessing black-hole binaries. II. A phenomenological model for the advanced detector era, Physical Review D **93**, 044007 (2016).

[45] S. Ossokine, A. Buonanno, S. Marsat, R. Cotesta, S. Babak, T. Dietrich, R. Haas, I. Hinder, H. P. Pfeiffer, M. Pürrer, C. J. Woodford, M. Boyle, L. E. Kidder, M. A. Scheel, and B. Szilágyi, Multipolar effective-one-body waveforms for precessing binary black holes: Construction and validation, Phys. Rev. D **102**, 044055 (2020), arXiv:2004.09442 [gr-qc].

[46] C. Talbot and E. Thrane, Gravitational-wave astronomy with an uncertain noise power spectral density, arXiv e-prints , arXiv:2006.05292 (2020), arXiv:2006.05292 [astro-ph.IM].

[47] K. Chatziioannou, C.-J. Haster, T. B. Littenberg, W. M. Farr, S. Ghonge, M. Millhouse, J. A. Clark, and N. Cornish, Noise spectral estimation methods and their impact on gravitational wave measurement of compact binary mergers, Phys. Rev. D **100**, 104004 (2019).

[48] D. Macleod, A. L. Urban, S. Coughlin, T. Massinger, M. Pitkin, paulaltin, J. Areeda, E. Quintero, T. G. Badger, L. Singer, and K. Leinweber, gwpy/gwpy: 1.0.1 (2020).

[49] G. Ashton, I. Romero-Shaw, C. Talbot, C. Hoy, and S. Galaudage, bilby pipe: 1.0.1 (2020).

[50] A. H. Nitz, T. Dent, G. S. Davies, S. Kumar, C. D. Capano, I. Harry, S. Mozzon, L. Nuttall, A. Lundgren, and M. Tápai, 2-OGC: Open Gravitational-wave Catalog of Binary Mergers from Analysis of Public Advanced LIGO and Virgo Data, ApJ **891**, 123 (2020), arXiv:1910.05331 [astro-ph.HE].

[51] A. H. Nitz, T. Dent, G. S. Davies, and I. Harry, A Search for Gravitational Waves from Binary Mergers with a Single Observatory, ApJ **897**, 169 (2020), arXiv:2004.10015 [astro-ph.HE].